AIAA 81-4008

Experimental Investigation of Conical Wall Jets

R. N. Sharma*
Indian Institute of Technology, Kanpur, India

The investigations described here pertain to the determination of the flowfields of different conical wall jet systems. The flow configuration is obtained by pushing a cone-frustum with a flow guide attached to its leading edge into a diffuser having the same included angle as the cone, creating a uniform gap. Air is blown through this gap along the conical surface to form a conical wall jet. A radial or cylindrical wall jet would occur if the apex angle α of the cone becomes 90 or 0 deg. A plane wall jet would occur if the radius of the cylinder becomes infinity for the case of $\alpha = 0$. The experimental results show that the dimensionless velocity profiles and the rate of jet spread follow patterns similar to those reported for a radial, plane, or cylindrical wall jet. Based upon available skin friction data for wall jets, the velocity profiles have been satisfactorily expressed in terms of variables in the law of the wall and the defect law. No effect of transverse curvature is observed. An analytical model based upon conservation of momentum in the axial direction has been developed to predict the longitudinal decay of the maximum velocity. The experimental data conform to the trends of the predictions.

Introduction

THE term "wall jet" was first introduced by Glauert.[1] It may be described as a jet blown over a surface through a slot. This type of flow configuration finds many uses in heat and mass transfer operations in a variety of industrial processes. The literature primarily reports the following types of wall jets:

1) Plane wall jet. This occurs when a jet, coming from a rectangular slit, is blown tangentially over a rigid surface. Thus, the angle of impingement of the jet on the surface is zero.

2) Radial wall jet. In this case the jet impinges normal to a flat surface and spreads out along the surface. The angle of impingement is 90 deg.

3) Cylindrical wall jet. This is created when a jet emerging from an annular slot flows longitudinally and coaxially along the surface of a cylinder.

Figure 1 illustrates the flow configurations of these jets.

An excellent survey on plane and radial wall jets is given by Spalding[2] and more recently by Rajaratnam.[3] Investigations on cylindrical wall jets have been reported by Lawrence,[4] Starr and Sparrow,[5] and Manian et al.[6] It is interesting to note that radial and plane wall jet flows exhibit strong similarities in many ways; for example, the angles of spread and the shape of the cross-stream velocity profiles are almost the same, yet the observed shear stress in the radial wall jet is twice as large as in the plane wall jet. That it should be so can be shown with the help of a simple momentum and mass balance across the boundary layer. The physical inquiry still remains as to why there should be an abrupt change in the shear stress values for the two cases. The idea to smooth this change resulted in the geometrical configuration of the present study.

A continuous geometric transition was conceived between the plane and radial wall jets where α, the angle between the flow direction and the axis of symmetry, changed continuously from 0 to 90 deg. This gave rise to a set of conical wall jets of which the previously mentioned wall jets become special cases. A conical wall jet can be defined as the jet blown through an annular slot along a conical surface. Thus, a cylindrical wall jet or a radial wall jet will occur if α is 0 or 90 deg. The cylindrical wall jet will reduce to a plane wall jet if the radius of the cylinder becomes very large. Figure 1 illustrates the geometrical implications of this point. Figure 2 describes a typical conical wall jet flow with the coordinate system used. The objective of the present experiments was to obtain data for various conical wall jet flows in terms of measuring mean velocity profiles at a number of longitudinal stations and subsequently to study them in the background of similar data for other reported wall jets.

Experiment

A general schematic diagram of the experimental setup is given in Fig. 3. A detailed description of the apparatus, test procedure, sources of error, and data reduction is reported in Ref. 7. Three centrifugal blowers, connected in series, were used to supply air. The issuing air from the last blower was conducted through a converging duct (reducer) into a mild steel pipe 7.6 cm in diameter and 4 m in length. A brass diffuser was attached to the other end of the pipe, which was properly supported and horizontally positioned. A hydraulically smooth wooden cone was properly suspended and pushed into this diffuser to the extent that a certain annular gap was left between the diffuser and the cone. The air from the pipe was blown through this annular gap (slot) along the surface of the cone as a wall jet in the way shown in Fig. 3. To avoid stagnation and sudden change of flow direction, a flow guide was attached at the leading edge of the cylinder and the cones which were already cut to a frustum with an initial diameter of approximately 16 cm. A 100×100

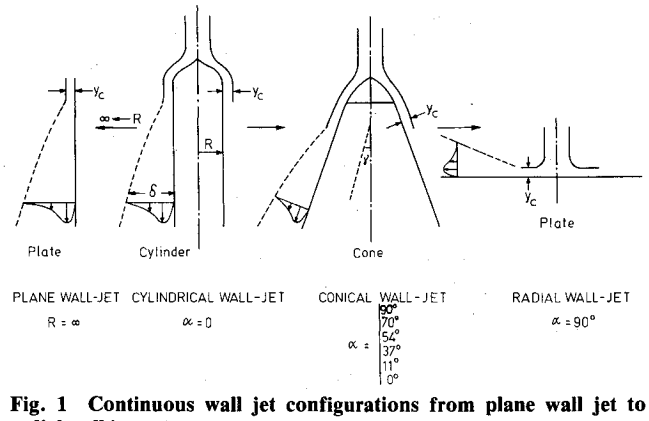

Fig. 1 Continuous wall jet configurations from plane wall jet to radial wall jet.

Received Sept. 28, 1979; revision received July 7, 1980. Copyright © American Institute of Aeronautics and Astronautics, Inc., 1980. All rights reserved.

*Dept. of Chemical Engineering; presently Visiting Professor, Swiss Federal Institute of Technology (ETH), Zurich, Switzerland.

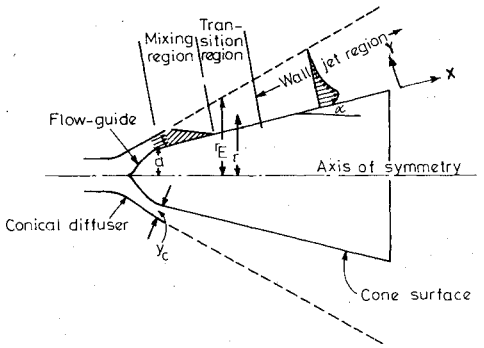

Fig. 2 Typical conical wall jet flow system.

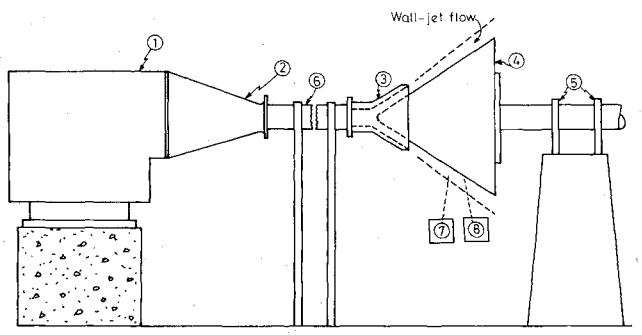

Fig. 3 General arrangement of the experimental setup.

cm rectangular plate of Perspex was used for the radial wall jet study. A flow guide was attached to it at the center.

In order to measure axial velocity profiles, a traversing unit was made, which carried a stainless-steel hypodermic tube (0.12 cm o.d., 0.077 cm i.d.) as the pitot probe. The cross-stream motion of the probe could be measured by a micrometer head to an accuracy of 0.001 cm, and the longitudinal positions of the probe could be recorded to an accuracy of 0.1 cm. A combination inclined/vertical manometer, connected differentially to the pitot probe, recorded the velocity pressure from which the magnitude of velocity was determined.

The plate or the cone with the corresponding diffuser was properly aligned so that the annular gap between the two could be set to a predetermined value. A check for the radial symmetry of the slot width was made by recording maximum velocity at four perpendicular positions for a specified axial distance. The slot width was adjusted until the manometer readings for the maximum velocities were identical. The traversing unit was aligned so that the probe could travel normal to the cone surface, and the unit as a whole slide parallel to the surface. Velocity profiles were thus obtained at a number of streamwise stations for various conical wall jet flows by measuring the velocity pressures at known positions of the probe normal to the main flow direction.

Results and Discussion

It has been observed that velocity profiles become fully developed beyond a region where $x/y_c > 20$. Results in this section pertain to fully developed velocity profiles.

Rate of Jet Spread

The rate of jet spread can be expressed as the variation of half-width $y_{1/2}$, which is a cross-stream distance corresponding to half of the maximum velocity u_{max} in any given axial velocity profile, with streamwise distance x from the slot. The published literature usually reports a linear rate of half-width growth and its value is variously given as between 0.06 and 0.085. This includes the data for radial, cylindrical, and plane wall jets. The half-width growth in the present experiments is also found to be approximately linear with the longitudinal distance, although closer scrutiny of the data shows that the jet spread in fact obeys a simple power law relation. For the sake of comparison with the reported data, a linear model is first assumed. The reported range of half-width growth for radial wall jets is between 0.06 and 0.08, and the values obtained from the present study satisfactorily lie between 0.06 and 0.071. It can be seen from Table 1 that the overall range of the rate of jet spread lies between 0.064 and 0.084 (except for flow systems corresponding to the smallest slot width used, i.e., y_c of the order of 0.1 cm). This, in general, is commensurate with the range of 0.06-0.085 for published investigations on radial, cylindrical, and plane wall jets.

Table 1 Jet spread rate

α, deg	y_c, cm	Re_c	Jet spread rate, $dy_{1/2}/dx$
11.25	0.102	0.3363×10^4	0.084
37.12	0.102	0.3115	0.100
53.92	0.103	0.3516	0.085
70.08	0.102	0.3622	0.088
90.00	0.099	0.3334	0.093
11.25	0.196	0.6474×10^4	0.077
37.12	0.196	0.6777	0.064
53.92	0.206	0.6098	0.068
70.08	0.196	0.6803	0.073
90.00	0.196	0.7022	0.071
0.0	0.302	0.5400×10^4	0.073
11.25	0.292	0.9645×10^4	0.084
37.12	0.315	0.1029×10^5	0.064
53.92	0.307	0.9784×10^4	0.068
70.08	0.306	0.1046×10^5	0.061
90.00	0.292	0.1026×10^5	0.060
0.0	0.579	0.1000×10^5	0.083
11.25	0.602	0.1733	0.075
37.12	0.621	0.1827	0.064
53.92	0.606	0.1816	0.068
70.08	0.635	0.1959	0.083
90.00	0.584	0.1904	0.083
11.25	1.262	0.2784×10^5	0.066
37.12	1.265	0.3168	0.074
53.92	1.273	0.3168	0.075
70.08	1.270	0.3346	0.078
90.00	1.257	0.3435	0.066

Plots of $y_{1/2}/y_c$ for slot widths on the order of 0.3 and 0.2 cm for all cone geometries are, respectively, shown in Figs. 4 and 5. Results of Myers et al.,[8] Jayatillaka,[9] Baker,[10] Starr and Sparrow,[5] Manian et al.,[6] and Subramanya[11] have also been plotted in the same figures. These data, as mentioned earlier, pertain to radial, cylindrical, and plane wall jets. It can be observed that the data of these authors agree satisfactorily with the experimental data of the present investigations. The rate of jet spread, therefore, seems to be independent of the nature of cone geometry α.

In Fig. 6, the $y_{1/2}/y_c$ vs x/y_c plot is shown for a typical cone geometry ($\alpha = 37$ deg) corresponding to five values of slot widths. The figure shows a slightly higher growth rate for the flow system corresponding to the smallest value of y_c; for the rest of the slot widths, it lies in the 0.060-0.084 limit. In fact, a close scrutiny of Fig. 7, which shows the jet spread for all of the flow systems excepting the ones with the smallest value of y_c (on the order of 0.1 cm), suggests that the magnitude of slot width does not affect the rate of jet spread. For low values of y_c, a higher rate of jet spread is observed. It is possible that there may be a slight dependence of the spread rate on y_c. The dependence is perceptible only for flow situations where the value of y_c is very low. Alternatively, the radial symmetry, which is difficult to obtain for small slot widths, might not have been achieved and, as such, the data may not be con-

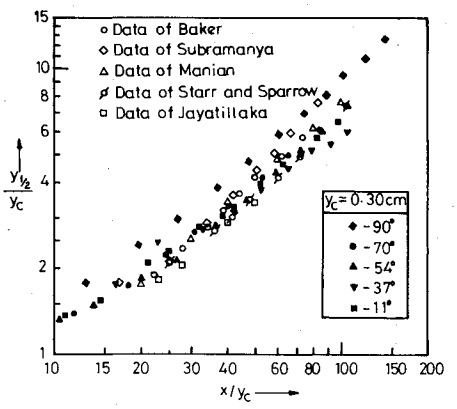

Fig. 4 Jet spread for all geometries (y_c constant).

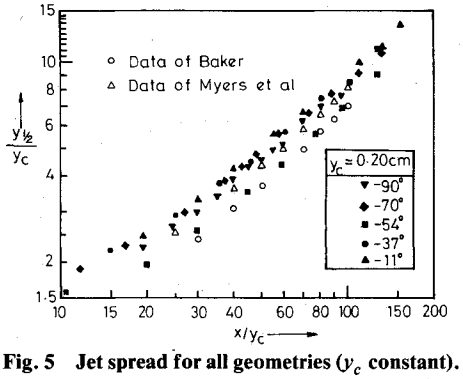

Fig. 5 Jet spread for all geometries (y_c constant).

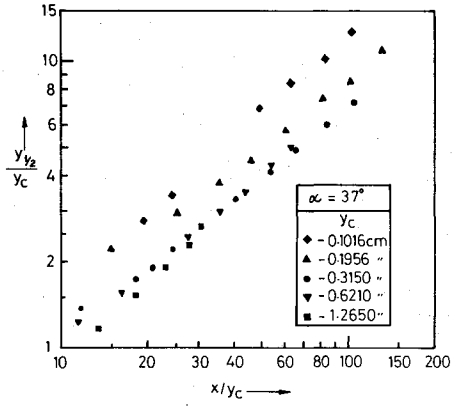

Fig. 6 Jet spread for different slot widths (α constant).

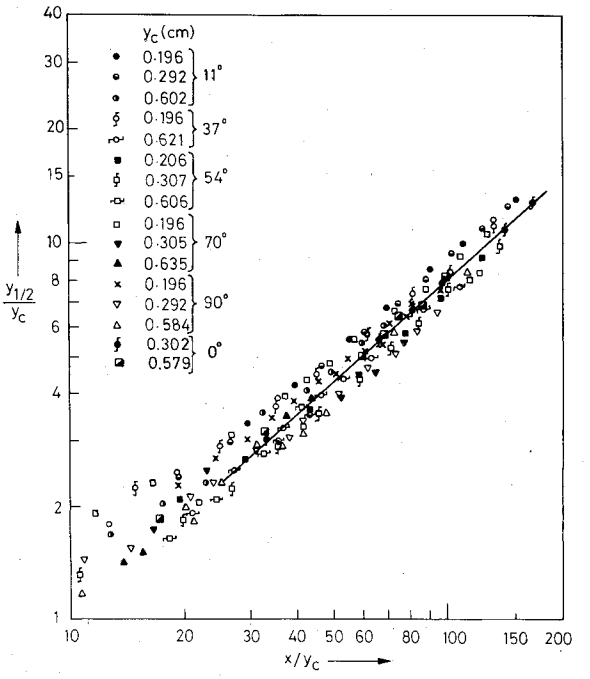

Fig. 7 Jet spread.

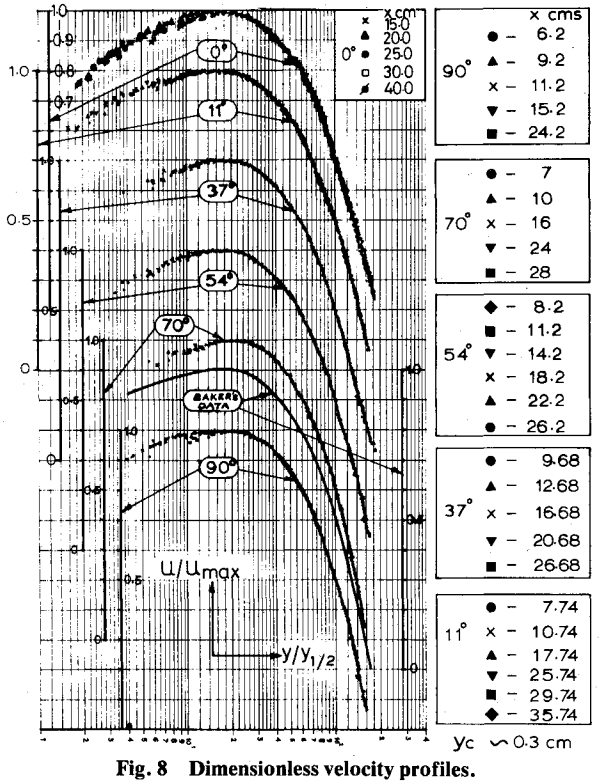

Fig. 8 Dimensionless velocity profiles.

sistent with corresponding data. A weak dependence of Reynolds number at the slot conditions Re_c on the wall jet growth has been predicted by Myers,[8] but no perceptible effect had been observed by the author or earlier workers.

Power Law Model for Jet Spread

The jet-spread data can be correlated by the power law expression:

$$y_{1/2}/y_c = A(x/y_c)^n \tag{1}$$

where x is often measured from a virtual origin, which is not generally coincident with the position of the slot. The value of A has been quoted differently, but almost all of the earlier investigators have reported the value of n as unity, which reduces the variation of $y_{1/2}$ with x as linear. Manian et al.[6] and more recently Narasimha and Narayan[12] have, respectively, reported the value of exponent n as 0.90 and 0.91. With a view to establishing the value of n from the present experiments, reference can be made to Fig. 7, where it can be seen that the jet spread obeys the simple power law relation:

$$y_{1/2}/y_c = 0.120(x/y_c)^{0.91} \tag{2}$$

It is interesting to compare this with a similar expression for cylindrical wall jets quoted by Manian et al.,[6] i.e.:

$$y_{1/2}/y_c = 0.125[(x+x_0)/y_c]^{0.90} \tag{3}$$

where x_0 is the distance of the virtual origin from the slot. Equations (2) and (3) compare excellently for large values of streamwise distance.

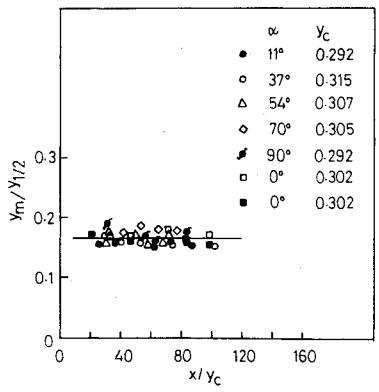

Fig. 9 Similarity of velocity profiles.

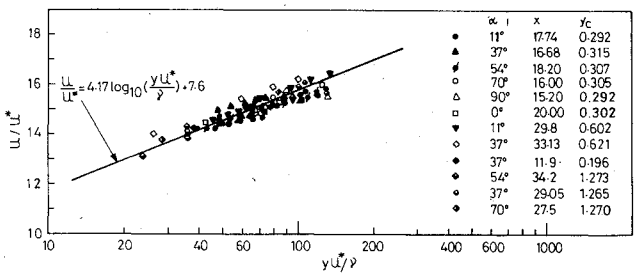

Fig. 10 Law of the wall representation of velocity data.

Velocity Profiles

Representative, fully developed dimensionless mean velocity profiles for conical wall jets corresponding to six cone angles with a slot width of the order of 0.3 cm are shown in Fig. 8. For comparison, the experimental velocity profile obtained by Baker[10] has also been drawn on the same figure. A close resemblance of the shapes of all of the velocity profiles is obvious. This implies that the shape of the dimensionless velocity profiles is independent of the nature of cone geometry α. In fact, when the velocity profiles for the rest of the flow systems were plotted (not shown), it was observed that the shape of velocity profiles was independent of the magnitude of slot width y_c as well. This similarity of velocity profiles had been observed earlier in plane and radial wall jet flows. Manian et al.[6] and Starr and Sparrow,[5] however, report the nonsimilar nature of these profiles in the region close to the wall which is the inner region where $y<y_m$ (y_m is the value of y corresponding to maximum velocity u_{max}), although according to them similarity persists in the outer region ($y>y_m$). They established the nonexistence of similarity in the inner region through a plot of $y_m/y_{1/2}$ as a function of x/y_c which departed significantly from a horizontal line that would have indicated similarity.

Present investigations indicate similarity of velocity profiles in both the inner and outer regions. It should be noted that the inner region could be explored only up to 0.06 cm from the wall due to limitations in probe size. Further evidence of the existence of similarity can be obtained by scrutinizing the thickness parameters y_m and $y_{1/2}$. Figure 9 is a plot of $y_m/y_{1/2}$ as a function of x/y_c for all cone geometries at a constant slot width on the order of 0.3 cm. A horizontal line suggests similarity. Additional data (not shown) show similar trends of a horizontal line, thereby establishing similarity of velocity profiles for all of the flow systems studied in the present investigations. The constant value of $y_m/y_{1/2}$ obtained from the present study is 0.17 while the corresponding value reported by Seban and Back[13] is 0.12. The only data available for conical wall jets are for specific cases of radial, plane, and cylindrical wall jets. The similarity of overall velocity profiles has been reported for radial and plane wall jets, conforming to similar results in the present work. In the case of cylindrical wall jets, however, the reported findings are at variance with the observations in the present study. The major difference between the earlier and present work is that the radii of the cylinders used in the two flow situations were different. Starr and Sparrow[5] used a 12.7 mm (½ in.) diameter rod, while Manian et al.[6] used 6.4 and 3.2 mm (¼ and ⅛ in.) diameter rods. The diameter of the cylinder as well as the initial radius of various cone geometries used in the present case centered around a value of 15 cm (6.0 in.), about 12 times more than the maximum diameter used by previous investigators. A parameter defining the curvatuve effects could be taken as δ/a, where δ is the local boundary-layer thickness and a is the initial radius of the conical geometry, which in the case of a cylinder reduces to its radius. Large values of δ/a would, it is anticipated, show pronounced curvature effects and the resulting velocity profiles would be nonsimilar until δ/a is so large that the influence of the bounding surface disappears and the flow configuration reduces to that of a free-circular jet and the similarity trends are regained. On the other hand, lower values of δ/a would reveal diminished curvature effects, until at some value the velocity profiles become similar. If this model of interpretation is true, then obviously the discrepancy between the two cited cases can be rationalized.

Table 2 Law of the wall ($u^+ = A\log_{10}y^+ + B$)

Author	A	B	Remarks
Bradshaw and Gee[15]	4.55	10.48	Still freestream
Mathieu[16]	5.07	9.84	
Kruka and Eskinazi[17]	4.42	9.00	Still freestream
	4.83	11.40	
Patel, R. P.[18]	4.14	9.10	
Patel, V. C.[19]	5.50	5.45	
Ramprian[20]	5.50	11.20	Wall jets in conical diffusers
Irwin[21]	5.50	5.45	
Present study	4.17	7.60	Conical wall jets in still freestream

Skin Friction, Law of the Wall, and Defect Law

The wall shear stress for wall jet flows is generally expressed in terms of a local friction coefficient C_{fm} defined as:

$$C_{fm} = \tau_s / \tfrac{1}{2}\rho u_{max}^2 \tag{4}$$

Shear stress data from plane wall jet experiments have been correlated by the following expression:

$$C_{fm} = A(Re_m)^{-m}; \quad Re_m = y_m u_{max}/\nu \tag{5}$$

Sigalla[14] reported the values of the constants A and m as 0.0565 and 0.25, respectively. Assuming no transverse curvature effects, it was thought worthwhile to use Sigalla's expression to process the velocity profiles of conical wall jet flows in terms of the law of the wall. The velocity data can be represented in terms of wall law variables in the form:

$$u^+ = f(y^+) \tag{6}$$

where u^+ and y^+, for a given velocity profile, can be calculated with the help of Eqs. (4) and (5). A semilog plot of these variables is shown in Fig. 10, which, from the law of the wall for conical wall jets, is found to be:

$$u/u^* = 4.17 \log_{10}(yu^*/\gamma) + 7.6 \tag{7}$$

Table 2 shows values of the law of the wall constants reported by several authors for wall jet flows.

The velocity distribution described by the law of the wall show a boundary-layer type similarity, yet the constants are

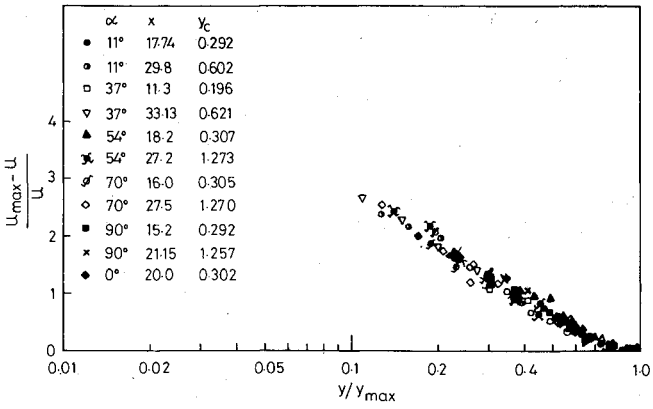

Fig. 11 Defect law representation of velocity data.

different from the boundary-layer case. Correlation of the velocity data by a representation of the defect law is shown in Fig. 11, where y has been normalized by y_m. Evidently, the correlation is satisfactory in the region $y/y_m > 0.1$.

Decay of Maximum Velocity

An analytical model predicting the longitudinal decay of maximum velocity can be developed by invoking the postulate of streamwise conservation of momentum, i.e., referring to coordinate system depicted in Fig. 2:

$$\mathrm{d}/\mathrm{d}x \int_0^\delta \rho u^2 2\pi r \mathrm{d}y = 0 \tag{8}$$

where r is given by:

$$r = a + x\sin\alpha + y\cos\alpha \tag{9}$$

where a is the initial radius of the cone. Therefore, equating the momentum at the slot to the momentum at any x:

$$\rho u_c^2 \int_a^{a+y_c\cos\alpha} 2\pi r \mathrm{d}r = \cos\alpha \int_{a+x\sin\alpha}^{a+x\sin\alpha+\delta\cos\alpha} \rho u^2 2\pi r \frac{\mathrm{d}r}{\cos\alpha} \tag{10}$$

Substituting the value of r and $\mathrm{d}r$ from Eq. (9) and assuming similarity of velocity profiles, i.e.:

$$u/u_{\max} = f(y/\delta) \tag{11}$$

Eq. (10) finally reduces to:

$$\frac{u_{\max}}{u_c} = \sqrt{\frac{a y_c [1 + (y_c\cos\alpha/2a)]}{(a + x\sin\alpha)\delta I_1 + \cos\alpha \delta^2 I_2}} \tag{12}$$

where

$$I_1 = \int_0^1 f^2 \mathrm{d}\eta; \quad I_2 = \int_0^1 \eta f^2 \mathrm{d}\eta; \quad \eta = (y/\delta) \tag{13}$$

The implication of Eq. (12) can now be examined for specific reported cases of conical wall jet flows with the prior knowledge that $\delta/x = c$, where c is a constant:

1) Radial wall jet ($\alpha = 90$ deg), for $x \gg a$

$$u_{\max}/u_c = \sqrt{a y_c / c I_1}\, x^{-1} \tag{14}$$

2) Plane wall jet ($\alpha = 0$, $a = \infty$)

$$u_{\max}/u_c = \sqrt{y_c / c I_1}\, x^{-1/2} \tag{15}$$

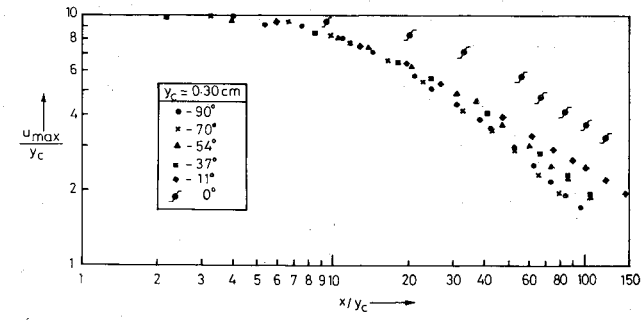

Fig. 12 Decay of maximum velocity for all cone geometries (y_c constant).

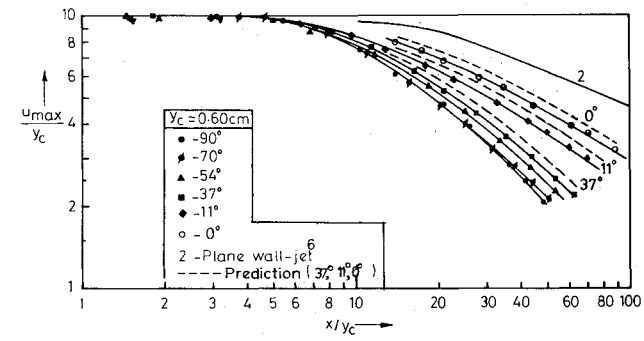

Fig. 13 Decay of maximum velocity for all cone geometries (y_c constant).

3) Free circular jet ($\alpha = 0$, $a = 0$)

$$\frac{u_{\max}}{u_c} = \sqrt{\frac{y_c^2/2}{c^2 I_2}}\, x^{-1} \tag{16}$$

4) Cylindrical wall jet ($\alpha = 0$)

$$\frac{u_{\max}}{u_c} = \sqrt{\frac{(y_c/a)(1 + [y_c/2a])}{(\delta/a) I_1 + (\delta^2/a^2) I_2}} \tag{17}$$

Starr and Sparrow[5] employed a similar analytical model wherein the wall effects are ignored, i.e., the momentum lost in the inner region is neglected. They used the following velocity profile to cover the whole region:

$$u/u_{\max} = \exp[-0.692 (y/y_{1/2})^2] \tag{18}$$

According to them:

$$\frac{u_{\max}}{u_c} = \frac{[(1/2)[r_N - a][r_N + a])/a^2]^{1/2}}{[0.361 (y_{1/2}/a)^2 + 0.753 (y_{1/2}/a)]^{1/2}} \tag{19}$$

where r_N is the nozzle exit radius. Also, $r_N - a = y_c$. Therefore, Eq. (19) can be written as:

$$\frac{u_{\max}}{u_c} = \sqrt{\frac{(y_c/a)(1 + [y_c/2a])}{[0.753 (y_{1/2}/a) + 0.361 (y_{1/2}/a)^2]}} \tag{20}$$

which is the same expression as Eq. (17) with δ, I_1, and I_2 evaluated in terms of $y_{1/2}$. From the present investigations $\delta = 2.0\, y_{1/2}$ while Starr and Sparrow[5] report a value of $2.3\, y_{1/2}$. It should be noted that with smaller values of δ/a (large a) the cylindrical wall jet reduces to a plane wall jet, as is obvious from Eq. (17) where $(\delta^2/a^2) I_2$ is neglected and the resulting expression corresponds to the plane wall jet equation (15). Therefore δ/a can, as earlier mentioned, be considered as a curvature parameter. Manian et al.[6] converted this parameter into $2a/y_c$.

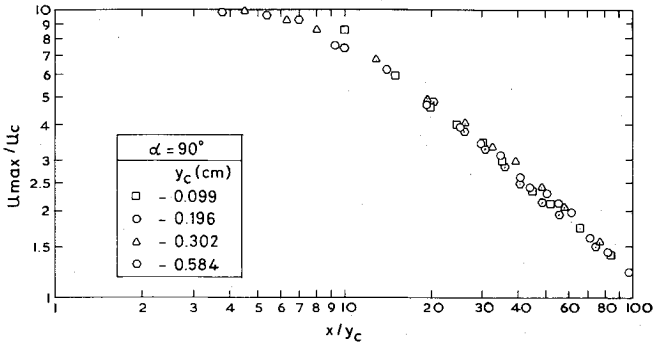

Fig. 14 u_{max} decay in radial wall jet.

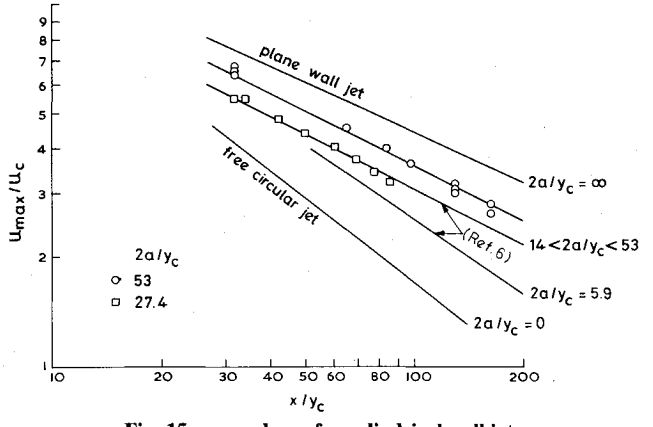

Fig. 15 u_{max} decay for cylindrical wall jets.

From the foregoing analysis it is clear that at large values of axial distances u_{max} decays linearly with x^b for two limiting cases, those of the plane wall jet ($b=-\frac{1}{2}$) and of the radial wall jet ($b=-1$). Figures 12 and 13 show the u_{max} decay for all cone geometries corresponding to y_c of the order of 0.3 and 0.6 cm, respectively. It can be seen that the u_{max} curve for intermediate cone geometries is confined between the above-mentioned limits. It can also be seen that u_{max} decreases faster with increasing values of α. As a further check on this trend, u_{max} variations for plane wall jet as reported by Manian et al.[6] are shown on Fig. 13. Predicted values of u_{max} decay with an assumed velocity profile as given by Eq. (18) are also shown in Fig. 13 on the basis of Eq. (12) which for this case can be approximated as:

$$\frac{u_{max}}{u_c}=\sqrt{\frac{ay_c[1+(y_c\cos\alpha/2a)]}{[0.753(a+x\sin\alpha)y_{1/2}+0.361y_{1/2}^2\cos\alpha]}} \qquad (21)$$

Qualitative agreement between the predicted and experimental values is obvious. The discrepancy can be attributed to the assumed velocity profile which is approximate in the sense that it does not cover the wall layer correctly.

Figure 14 describes longitudinal variations of u_{max} in radial wall jet as a function of x/y_c for different values of slot widths. The data points follow a common curve, the slope of which at large axial distances is approximately unity, confirming the trends predicted by Eq. (14). The parametric dependence of $2a/y_c$ seems to be insensitive to the decay curve.

Figure 15 represents the data points of the present experiments for cylindrical wall jets together with those reported by Manian et al.[6] For a value of $2a/y_c$ equal to 27.6, the points of the present study lie on the curve which has the range $14<2a/y_c<53$. The curve corresponding to $2a/y_c=53$ is shifted upward. The present data seem to fit in the picture of u_{max} decay as described by Manian et al.[6]

Conclusions

Conical wall jets successfully bridge the gap between the radial and plane wall jets through continuous transition of the half-angle α of the cone in the range of 0-90 deg. In the far downstream region ($x/y_c>20$):

1) The jet spread obeys a simple power law relation which does not depend on the nature of the cone geometry. The relation therefore defines the jet spread for all specific cases of conical wall jets which include radial, cylindrical, and plane wall jets.

2) The velocity profiles are similar in both the inner and outer regions. Based upon available skin friction data, the velocity profiles have been satisfactorily expressed in terms of wall and defect law variables. Transverse curvature effects were not observed.

3) On the basis of conservation of momentum in the axial direction, an analytical expression is developed which satisfactorily accounts for u_{max} decay in conical wall jets.

References

[1] Glauert, M. B., "The Wall Jet," *Journal of Fluid Mechanics*, Vol. 1, 1956, pp. 625-643.

[2] Spalding, D. B., *Lecture in Mathematical Models of Turbulence*, Academic Press, London, 1972.

[3] Rajaratnam, N., *Turbulent Jets*, Elsevier, New York, 1976.

[4] Lawrence, R. L., "Velocity Profiles from Compressible Wall Jets," *AIAA Journal*, Vol. 2, 1964, p. 574.

[5] Starr, J. B. and Sparrow, E. M., "Experiments on a Turbulent Cylindrical Wall Jet," *Journal of Fluid Mechanics*, Vol. 29, 1967, pp. 495-512.

[6] Manian, V. S., McDonald, T. W., and Beasant, R. W., "Heat Transfer Measurements in Cylindrical Wall Jets," *International Journal of Heat and Mass Transfer*, Vol. 12, 1969, pp. 673-679.

[7] Sharma, R. N., "Momentum and Mass Transfer in Turbulent Conical Wall Jets," Ph.D. Thesis, Dept. of Chemical Engineering, Indian Institute of Technology, Kanpur, India, 1972.

[8] Myers, G. E., Schauer, J. J., and Eustis, R. H., "Heat Transfer to Plane Turbulent Wall Jets," ASME Paper 62-HT-33, 1962.

[9] Jayatillaka, C.L.Y., "The Influence of Prandtl Number and Surface Roughness on the Resistance of the Laminar Sub-Layer to Momentum and Heat Transfer," Imperial College, London, Rept. TWF/R/2, 1967.

[10] Baker, E., "Influence of Mass Transfer on Surface Friction at a Porous Surface," Ph.D. Thesis, Faculty of Engineering, University of London, London, 1967.

[11] Subramanya, A. R., "Effects of Surface Roughness on Hydrodynamic and Thermal Boundary Layers," M. Tech. Thesis, Dept. of Mechanical Engineering, Indian Institute of Technology, Kanpur, India, 1969.

[12] Narashimha, R., Yegna Narayan, K., and Parthasarathy, S. P., "Parametric Analysis of Turbulent Shear Flows," *Aeronautical Journal*, Vol. 77, 1973, p. 355.

[13] Seban, R. A. and Back, L. H., "Velocity and Temperature Profiles in a Wall Jet," *International Journal of Heat and Mass Transfer*, Vol. 3, 1961, p. 225.

[14] Sigalla, A., "Measurements of Skin Friction in a Plane Turbulent Wall Jet," *Journal of the Royal Aeronautical Society of London*, Vol. 62, 1958, pp. 873-877.

[15] Bradshaw, P. and Gee, M. T., "Turbulent Wall Jets with and without External Stream," *Aeronautical Research Council*, R&M 3252, 1962.

[16] Mathieu, J., "Contribution à l'étude aerothermique d'un jet plan évaluent en présence d'une paroi," *Publications Scientifiques et Techniques du Ministère de l'Air*, No. 374, 1964.

[17] Kruka, V. and Eskinazi, S., "The Wall Jet in a Moving Stream," *Journal of Fluid Mechanics*, Vol. 29, 1964, pp. 555-579.

[18] Patel, R. P., "Self-Preserving Two-Dimensional Turbulent Jets and Wall Jets in a Moving Stream," M. Thesis, McGill University, Montreal, Canada, 1962.

[19] Patel, V. C., "Calibration of the Preston Tube and Limitations on Its Use in Pressure Gradients," *Journal of Fluid Mechanics*, Vol. 23, 1965, p. 185.

[20] Ramaprian, B. R., "Turbulent Wall Jets in Conical Diffusers," *AIAA Journal*, Vol. 11, 1973, pp. 1684-1690.

[21] Irwin, H.P.A.H., "Measurements in a Self-Preserving Plane Wall Jet in a Positive Gradient," *Journal of Fluid Mechanics*, Vol. 61, 1973, p. 33.